Study of the Extinction Coefficients of Single-Walled Carbon Nanotubes and Related Carbon Materials

B. Zhao, M. E. Itkis, S. Niyogi, H. Hu, J. Zhang, and R. C. Haddon*

Center for Nanoscale Science and Engineering, Departments of Chemistry and Chemical & Environmental Engineering, University of California, Riverside, California 92521-0403

Received: November 7, 2003; In Final Form: February 14, 2004

The measurement of the bulk purity of single-walled carbon nanotubes (SWNTs) is an important outstanding problem. We report a solution-phase near-IR (NIR) spectroscopic study of a range of carbon materials with an emphasis on SWNTs, and we show that NIR spectroscopy is an extremely powerful tool in the assessment of the carbonaceous purity of SWNTs. We demonstrate the applicability of Beer's law for all of the carbon materials included in this study within a range of concentrations in dimethylformamide (DMF), and we are able to solve for the effective extinction coefficients. By analyzing the areal absorptivities of the second interband transition of semiconducting SWNTs for a number of samples of differing purities, we are able to derive an absolute molar extinction coefficient for the carbonaceous impurities in SWNT samples. We demonstrate significant progress toward the establishment of an absolute scale for the bulk carbonaceous purity of SWNTs.

Introduction

The purification of carbon nanotubes (CNTs) is a vital area of current research within the larger effort of CNT manufacture. For electric arc (EA)-produced single-walled carbon nanotubes (SWNTs), metal catalysts, amorphous carbon, and graphitic nanoparticles are the major impurities. The existence of these impurities has hindered the widespread applications of SWNTs. A large number of purification methods have been reported, but the evaluation of the purity of SWNTs still represents a major challenge.

Several methods, including scanning electron microscopy (SEM),[1−7] transmission electron microscopy (TEM),[2,6,8,9] atomic force microscopy (AFM),[4,10] thermogravimetric analysis (TGA),[2,4,6,8,11,12] and Raman spectroscopy,[1,2,4−6,10,12] have been employed to evaluate the purity of SWNTs. In some cases, the purity of the SWNTs was reported to be higher than 90%.[1,5,8,13] Recently, a method to quantitatively evaluate the purity of as-prepared (AP-) SWNT soot by the use of solution-phase near-IR spectroscopy (NIR) has been reported by our group, in which the SWNT purity was evaluated against a reference sample by using the region of the second interband transition (S_{22}, with spectral cutoffs of SCL = 7750 and SCH = 11 750 cm^{-1}) for semiconducting SWNTs.[14] This method of relative purity determination requires calibration against a reference sample. In this paper, we report the study of the absolute extinction coefficients of EA-produced SWNTs and other carbon materials by the use of solution-phase NIR spectroscopy. We report significant progress toward the determination of the absolute purity of SWNTs.

Experimental Section

EA-produced as-prepared SWNTs are denoted EA-AP, whereas EA-purified SWNTs are denoted EA-P. Samples EA-AP2 and EA-AP5 (purity 30−50%) were obtained from Carbon Solutions, Inc; sample EA-AP6 was purchased from Carbolex, Inc. (purity 50−70%); carbon black (CB) was purchased from Alfa Aeser; multiwalled carbon nanotubes (MWNTs) were purchased from Nanolab (hollow structure, 95% purity); SWNTs produced by the HiPco method (HC-SWNT) were purchased from Carbon Nanotechnologies Inc.; SWNTs produced by the laser oven method (LO-SWNT) were obtained from Rice University (tubes@rice). All other reagents were purchased from Aldrich and used as received. The solution-phase NIR spectra were measured with a Varian Cary 500 IR-Vis-UV spectrometer. TGA data were recorded using a Perkin-Elmer Instruments Pyris Diamond TG/DTA thermogravimetric/differential thermal analyzer, with a heating rate of 5 °C/min in air.

The dispersion samples of the carbon materials were prepared as follows: 10.00 mg (±0.05 mg) of material was weighed and then sonicated in 50.0 mL (±0.1 mL) of DMF for 30 min to give a dispersion of concentration 0.2 mg/mL. Dispersion samples with other concentrations (0.1, 0.05, 0.02, 0.01, and 0.005 mg/mL) were prepared by diluting the 0.2 mg/mL dispersion with fresh DMF and sonicating for an additional 10 min. NIR spectra were recorded immediately after the samples were fully dispersed; representative spectra of the different carbon materials are shown in Figure 1 at a concentration of 0.01 mg/mL.

Analysis

The interband electronic transitions provide the spectroscopic signature of the SWNTs.[14,15] Figure 2a shows a NIR−Vis spectrum of an EA-AP sample in a DMF dispersion. We chose this solvent because SWNTs can be dispersed in DMF by ultrasonication at reasonable concentrations without appreciable damage to the SWNTs.[16,17] Furthermore, DMF is transparent

* Corresponding author. E-mail: haddon@ucr.edu.

10.1021/jp037402o CCC: $27.50
Published on Web 05/21/2004

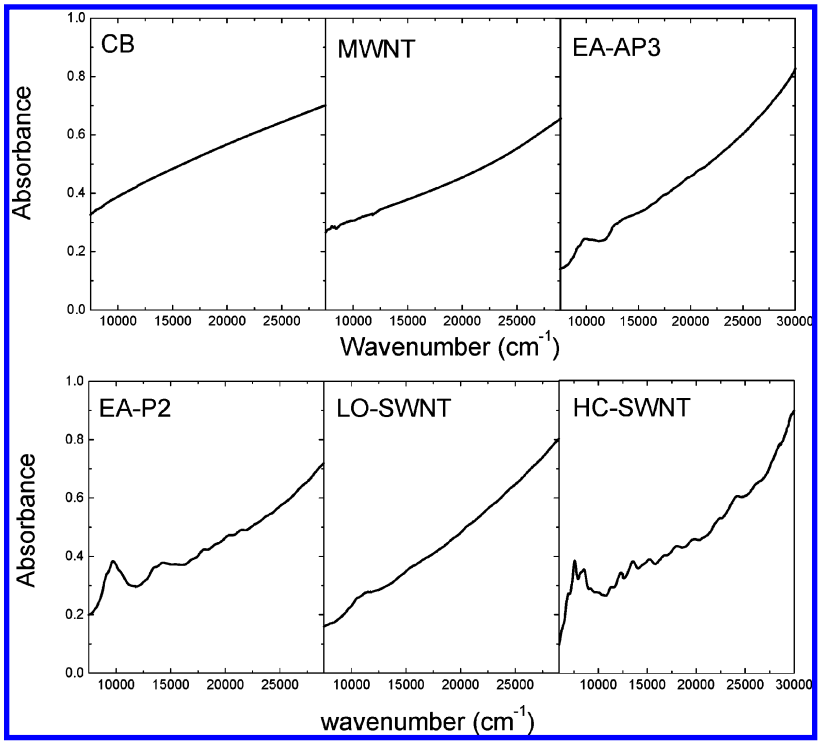

Figure 1. Representative spectra of carbon materials included in this study at a concentration of $C = 0.01$ mg/mL in DMF.

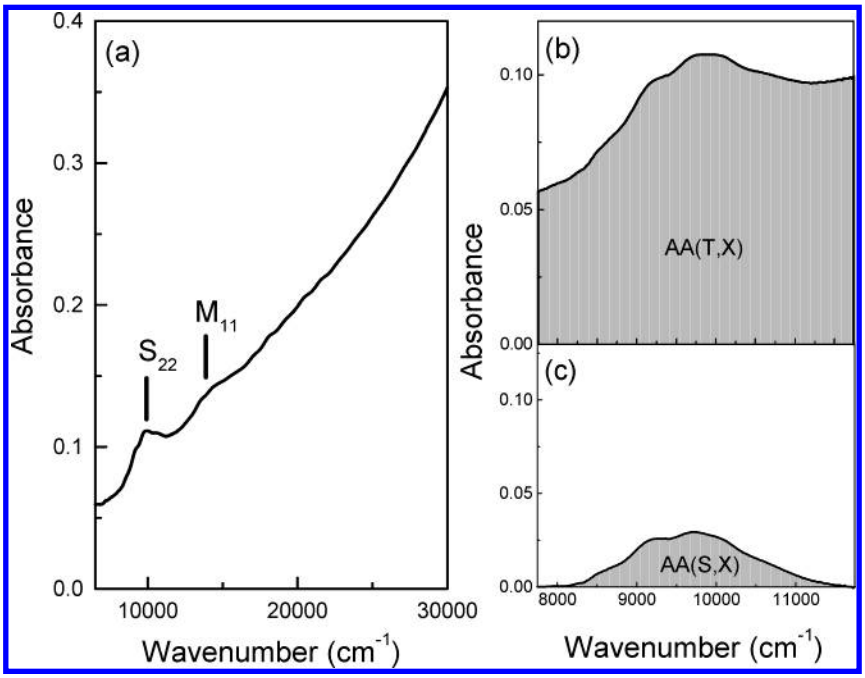

Figure 2. (a) NIR−vis spectrum of EA-produced AP-SWNT in DMF solution (0.01 mg/mL), (b) NIR spectrum in the region of the S_{22} interband transition (spectral cutoffs of SCL = 7750 and SCH = 11 750 cm^{-1}), and (c) after baseline correction.

in the 7500−35 000 cm^{-1} spectral range, which allows the observation of the S_{22} and M_{11} interband transitions for EA-SWNTs.[14] The peaks centered at 9800 cm^{-1} are due to transitions between the second pair of singularities in the density of states (DOS) of the semiconducting SWNTs (S_{22}), and the peaks centered at 13 800 cm^{-1} are due to the first pair of singularities in the DOS of metallic SWNTs (M_{11}).[15] The first pair of singularities in the DOS of the semiconducting SWNTs (centered at 5450 cm^{-1}, S_{11}) is masked by the solvent absorption; thus, the S_{22} absorption is used to analyze the SWNT content of the sample.[14]

In our previous work,[14] the relative purity (RP) of a SWNT sample X was estimated by comparison to a high-purity reference SWNT sample (R):

$$\mathrm{RP(X)} = \frac{[AA(\mathrm{S, X})/AA(\mathrm{T, X})]}{[AA(\mathrm{S, R})/AA(\mathrm{T, R})]} \quad (1)$$

$$= \frac{[A(\mathrm{S, X})/A(\mathrm{T, X})]}{[A(\mathrm{S, R})/A(\mathrm{T, R})]} \quad (2)$$

in which the *AA* values (areal absorbance) are obtained by integrating the NIR spectra between the spectral cutoffs of SCL

TABLE 1: Abbreviations Used in This Paper

SWNT	single-walled carbon nanotubes
AP-EA	as-prepared SWNTs (electric arc method)
P-EA	purified SWNTs (electric arc method)
LO-SWNT	as-prepared SWNTs (laser oven method)
HC-SWNT	as-prepared SWNTs (HiPCO method)
MWNT	multiwalled carbon nanotubes
CB	carbon black
SCL	spectral cutoff at low frequency (cm^{-1})
SCH	spectral cutoff at high frequency (cm^{-1})
RP	relative purity
AA(S)	areal absorbance of SWNT interband transition
AA(T)	total areal absorbance
AA(N)	areal absorbance of SWNT π-plasmon
AA(I)	areal absorbance of carbonaceous impurities
A(S)	effective absorbance of SWNT interband transition
A(T)	total effective absorbance
A(I)	effective absorbance of carbonaceous impurities
A(N)	effective absorbance of SWNT π-plasmon
PI	pure carbonaceous impurity sample
PN	pure SWNT sample (electric arc method)
C(X)	total carbonaceous concentration of sample X (moles of carbon L^{-1})
C(W, X)	SWNT concentration of sample X (moles of carbon L^{-1})
C(I, X)	carbonaceous impurities concentration of sample X (moles of carbon L^{-1})
ϵ(T)	extinction coefficient of total carbonaceous materials ($L\ mol^{-1}\ cm^{-1}$)
ϵ(N)	extinction coefficient of SWNT π-plasmon ($L\ mol^{-1}\ cm^{-1}$)
ϵ(S)	extinction coefficient of SWNT S_{22} interband transition ($L\ mol^{-1}\ cm^{-1}$)
ϵ(I)	extinction coefficient of carbonaceous impurities ($L\ mol^{-1}\ cm^{-1}$)

$= 7750$ and SCH $= 11\,750\ cm^{-1}$ (chosen to capture the S_{22} interband transition for EA-SWNTs). *AA*(T, X) is the total area under the S_{22} interband transition, whereas *AA*(S, X) is the area under the S_{22} absorption after baseline correction (Figure 2b and c; note the change in notation from the initial work,[14] where the areal absorption was previously denoted by *A*). *A*(S) and *A*(T) are the effective absorbencies and are obtained by dividing *AA*(S) and *AA*(T) by the spectral width used in the integration (SCH − SCL $= 4000\ cm^{-1}$). The choice of spectral cutoffs is crucial and according to a referee may fail to capture some of the intensity of the S_{22} component due to transitions arising from the joint density of states.

In eqs 1 and 2, the ratio of *A*(S, R)/*A*(T, R) $= 0.141 =$ *AA*(S, R)/*AA*(T, R), where R = R2, the reference sample utilized previously.[14] The areal absorbance (*AA*) and the effective absorbance (*A*) of all of the samples are listed in Table 2. The relative purities of the EA-AP(1−6) and purified EA-P(1−3) reflect the SWNT content of the sample as a percentage of carbon in the samples. In the case of EA-P(1−3), the relative purity is more than 100%, which indicates that the content of SWNTs in these materials is higher than that of R2.[14] SEM images of EA-P1 and EA-P2 confirm the high purity of these EA-SWNTs (Figure 3).Thus, the purity of R2 is still below the value of the ideal pure SWNT sample.[14] Hence, the ratio of *A*(S)/*A*(T) for pure SWNTs, which is the key to the estimation of the purity of SWNT samples, must be larger than the value of 0.141 found previously for a high-purity sample of EA-SWNTs.[14]

For EA-SWNTs, the contaminants include metal catalysts, amorphous carbon, and carbon nanoparticles. To obtain an accurate relationship between the concentration of carbon in the samples and their absorption, the weight of metal in the samples must be subtracted from the total weight of the sample to correct the carbon concentration. TGA was used to estimate the weight of metal by ramping the temperature of the sample to 1000 °C in air, which leaves the residue in the form of metal oxides. After subtracting the weight of oxygen present in the residue (which usually constitutes about 21% of the final weight of the metal oxide), the exact weight of metal present in the original sample can be obtained. After correction for metal, the total concentration, *C*(X), of the carbonaceous components in a dispersion-phase sample X is equal to the sum of the concentrations of the SWNTs (W) and the carbonaceous impurities (I):

$$C(\mathrm{X}) = C(\mathrm{W, X}) + C(\mathrm{I, X}) \tag{3}$$

Figure 4 is a schematic illustration of the determination of the *AA* values within an integration range of SCL = 7750 and SCH $= 11750\ cm^{-1}$ for a (hypothetical) pure carbonaceous impurity sample (PI, Figure 4a), a (hypothetical) pure SWNT sample (PN, Figure 4b), and an arbitrary SWNT sample (X, Figure 4c), where S refers to the S_{22} interband transition of SWNTs. N and I refer to the background carbon π-plasmon absorption in the SWNTs and the carbonaceous impurities, respectively. According to Beer's law, the relationship of the effective absorbencies (*A*) and the concentrations (*C*, moles of carbon/L) can be expressed as

$$A = \epsilon \times C \times l \tag{4}$$

where ϵ is the molar extinction coefficient ($L \times mol^{-1} \times cm^{-1}$) and *l* is the path length of the spectroscopic cuvette (1 cm in the present work).

$$A(\mathrm{I, X}) = \epsilon(\mathrm{I}) \times C(\mathrm{I, X}) \times l \tag{5}$$

$$A(\mathrm{N, X}) = \epsilon(\mathrm{N}) \times C(\mathrm{W, X}) \times l \tag{6}$$

$$A(\mathrm{S, X}) = \epsilon(\mathrm{S}) \times C(\mathrm{W, X}) \times l \tag{7}$$

With this partitioning, the total absorbance (T) of an arbitrary SWNT sample is equal to the sum of the absorbance due to the S_{22} interband transition of the SWNTs (S), the background π-plasmon transition of the SWNTs (N), and the background π-plasmon transition of the impurities (I).

$$A(\mathrm{T, X}) = A(\mathrm{I, X}) + A(\mathrm{N, X}) + A(\mathrm{S, X}) \tag{8}$$

From the preceding equations, we can obtain the following relationships (in which we have set *l* equal to unity):

$$A(\mathrm{T, X}) = \epsilon(\mathrm{I}) \times C(\mathrm{I, X}) + [\epsilon(\mathrm{N}) + \epsilon(\mathrm{S})] \times C(\mathrm{W, X}) \tag{9}$$

$$A(\mathrm{T, X}) = \epsilon(\mathrm{I}) \times C(\mathrm{X}) + \{[\epsilon(\mathrm{N}) + \epsilon(\mathrm{S}) - \epsilon(\mathrm{I})] \times \epsilon(\mathrm{S})^{-1}\} \times A(\mathrm{S, X}) \tag{10}$$

Thus, for a series of SWNT samples of varying purity that are prepared to give solutions of the same total carbon concentration [*C*(X)], there should be a linear relationship between *A*(T, X) and *A*(S, X), and thus a plot of these two quantities should give a straight line with gradient $\{[\epsilon(\mathrm{N}) + \epsilon(\mathrm{S}) - \epsilon(\mathrm{I})] \times \epsilon(\mathrm{S})^{-1}\}$ and intercept $\epsilon(\mathrm{I}) \times C(\mathrm{X})$, thereby allowing the immediate determination of ϵ(I), the absolute extinction coefficient of the impurities present in EA-SWNTs.

Results and Discussion

To proceed with the analysis outlined above, it is necessary to test the applicability of Beer's law; Figure 5 shows a plot of concentration versus the absorbance/concentration data of the carbon materials included in this study. The absorbance

TABLE 2: Weight of Metal and Areal Absorbance of SWNTs and Carbon Materials

sample	wt % of metal[a]	*AA*(S)[b]	*AA*(T)[b]	*A*(S)[c]	*A*(T)[c]	*A*(T) − *A*(S)	purity (% of R-SWNT)
EA-AP1[d]	22.9	103.06	1162.92	0.026	0.291	0.265	63.4
EA-AP2[d]	30.7	51.13	980.22	0.013	0.245	0.232	37.6
EA-AP3[d]	27.4	115.50	1178.06	0.029	0.295	0.266	69.7
EA-AP4[d]	34.4	13.98	909.74	0.003	0.227	0.224	9.4
EA-AP5[d]	38.7	62.37	1135.09	0.016	0.284	0.268	40.0
EA-AP6[d]	28.3	43.47	971.58	0.011	0.243	0.232	32.1
EA-P1[d]	13.8	150.33	920.47	0.038	0.230	0.192	117.2
EA-P2[d]	8.7	253.57	1354.75	0.063	0.339	0.276	131.8
EA-P3[d]	4.5	209.43	1308.13	0.052	0.327	0.275	112.8
CB[d]	0.0		1452.99		0.363		
MWNT[d]	2.7		1247.19		0.312		
HC-SWNT(S_{11})[e]	14.8	534.35	1701.77	0.100	0.318	0.218	
HC-SWNT(S_{22})[f]	14.8	142.37	2110.92	0.028	0.411	0.383	
LO-SWNT[g]	14.8	73.57	1474.82	0.015	0.295	0.280	

[a] The weight of metal has been corrected by normalization for the formation of metal oxides. [b] The concentration of samples is 0.01mg/mL in DMF. [c] $A(S) = AA(S)/(SCH - SCL)$ and $A(T) = AA(T)/(SCH - SCL)$, where SCH and SCL are the high and low values of the spectral cutoffs used for the integration of the absorbance. [d] Spectral cutoffs: SCL = 7750 and SCH = 11 750 cm^{-1}. [e] Spectral cutoffs: SCL = 5400 and SCH = 10 750 cm^{-1}. [f] Spectral cutoffs: SCL = 10750 and SCH = 15 900 cm^{-1}. [g] Spectral cutoffs: SCL = 8380 and SCH = 13 380 cm^{-1}.

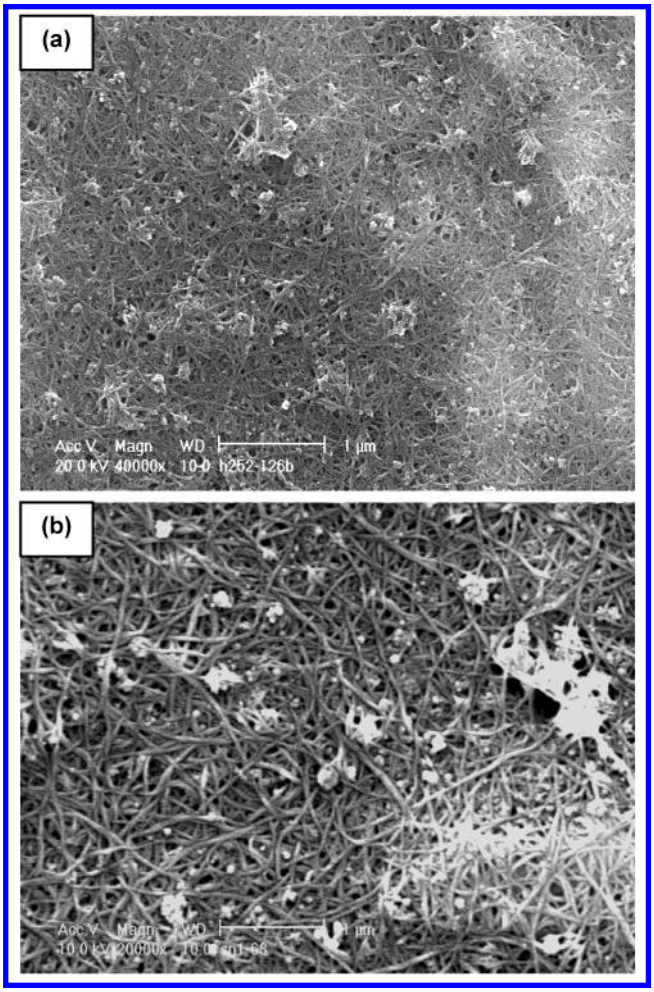

Figure 3. SEM images of (a) EA-P1 and (b) EA-P2.

measurements of all of the samples are taken at 7750 cm^{-1} (10 750 cm^{-1} for HC-SWNT), and the concentrations are 0.10, 0.05, 0.02, 0.01, and 0.005 mg/mL. The absorbance at this wavenumber does not include the absorbance from the interband transitions of SWNTs. Therefore, this absorbance results from the π-plasmons bands of the SWNTs and carbonaceous impurities. From the plot, we conclude that the samples obey Beer's law, at least for concentrations of 0.05, 0.02, and 0.01 mg/mL. Thus, we chose samples with concentrations of 0.02 and 0.01 mg/mL for further analysis. The data for the HC-SWNTs do not give a linear relationship (Figure 6), and this is related to the difficulty in obtaining stable dispersions of this material in DMF.[17]

On the basis of the applicability of Beer's law, we can estimate the effective extinction coefficient of solutions of the carbon materials. Table 3 lists the effective molar extinction coefficients of the solutions, in which ϵ(S) represents the extinction coefficient of the S_{22} interband transition of the SWNTs whereas ϵ(T) represents the total extinction coefficient. It is found that the extinction coefficients per mole of carbon for the materials included in this study fall in the range of $\epsilon(T) = 260-490$ L mol^{-1} cm^{-1}. This result is comparable to a previous report on functionalized materials.[18] For HC-SWNTs, an extinction coefficient of $\epsilon = 343$ L mol^{-1} cm^{-1} (in our units) at 500 nm has been reported in dichlorobenzene:[19] we find $\epsilon =$ 420 L mol^{-1} cm^{-1} for HC-SWNTs at this wavelength in DMF. An examination of all of the samples in the spectral range between 0.5 and 5 eV shows that the frequency dependence of the extinction coefficients is remarkably constant, given the diversity of carbon materials included in this study (Figure 1). On the basis of previous thin-film studies,[15] we estimate the maximum extinction coefficient for all of these carbon materials to be $\epsilon(T)_{max} \approx 2500$ L mol^{-1} cm^{-1} at ~5 eV. For aromatic molecules such as benzene, the $\pi \rightarrow \pi^*$ transitions are usually characterized by high molar absorptivity with $\epsilon_{max} \approx 10^5$ L mol^{-1} cm^{-1}. To compare with the SWNTs, however, this value would have to be normalized by the number of carbon atoms and thus would be reduced by about an order of magnitude. Comparing our results with the extinction coefficients of aromatic hydrocarbons is not straightforward. For example, annelation does not increase the extinction coefficient of polycyclic hydrocarbons, although the electronic transitions are generally shifted to lower energy.[20] The molar extinction coefficient of a 100-nm-long SWNT in which all 16 000 carbon atoms[21] are included in the molecular weight would have a value of $\epsilon \approx 10^7$ L mol^{-1} cm^{-1} in the NIR part of the spectrum.

Figure 6 shows the plot of concentration versus absorbance/concentration taken at 9850 cm^{-1} (7560 cm^{-1} for HC-SWNT S_{11}, 13 450 cm^{-1} for HC-WNT S_{22}, 10 450 cm^{-1} for LO-SWNT S_{22}), where these absorbencies correspond to the peak of the S_{22} interband transition of EA-SWNTs. The ratio of absorbance decreases in the following order: HC(S_{11}) > EA-P2 > CB > HC(S_{22}) > MWNT > EA-P1 > EA-AP1 > LO > EA-AP2 > EA-AP4. This order bears a relationship to the purity of EA-

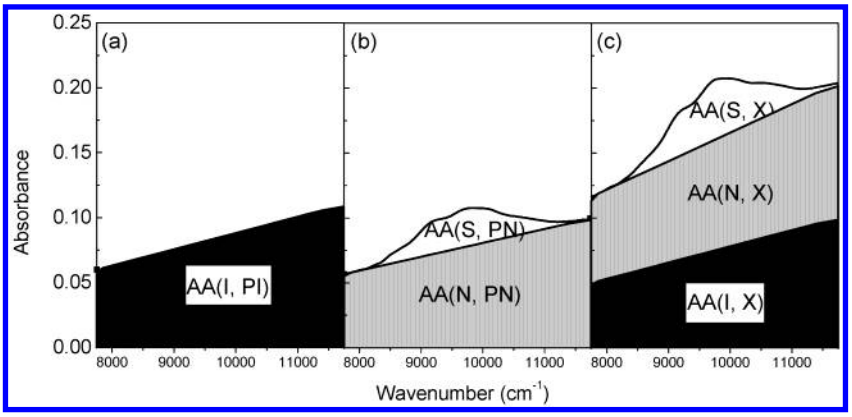

Figure 4. Schematic illustration of the areal absorption of hypothetical samples in the region of the S_{22} interband transition of EA-SWNTs (spectral cutoffs of SCL = 7750 and SCH = 11 750 cm^{-1}) for (a) a pure impurity sample, (b) a pure SWNT sample, and (c) an arbitrary SWNT sample.

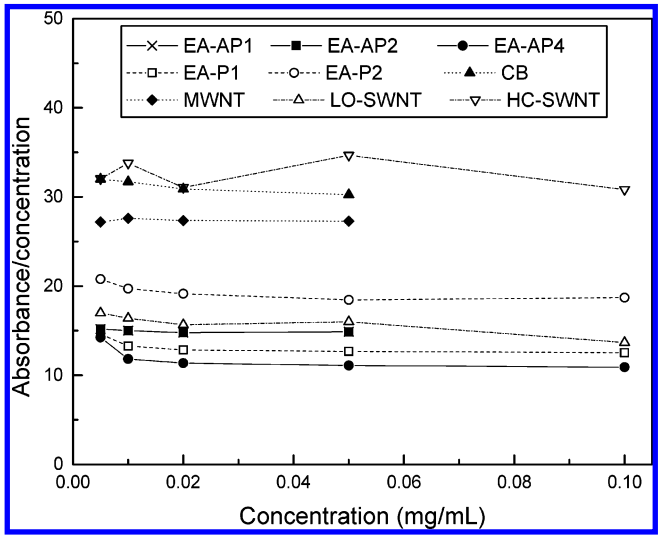

Figure 5. Plot of concentration versus absorbance (at 7750 cm^{-1}; 10 750 cm^{-1} for HC-SWNT) for the carbon materials.

TABLE 3: Effective Extinction Coefficients of Carbon Materials (Data from Table 2)

sample	ϵ(S)[a] (L mol^{-1} cm^{-1})	ϵ(T)[a] (L mol^{-1} cm^{-1})	ϵ(T) − ϵ(S) (L mol^{-1} cm^{-1})
EA-AP1	31	351	319
EA-AP2	16	295	280
EA-AP3	35	355	320
EA-AP4	4	273	270
EA-AP5	19	342	323
EA-AP6	13	293	280
EA-P1	46	277	231
EA-P2	76	408	333
EA-P3	63	394	331
CB		437	
MWNT		376	
HC-SWNT(S_{11})	120	383	263
HC-SWNT(S_{22})	34	495	461
LO-SWNT	18	355	337

[a] Note that these extinction coefficients are based on the total molar concentration of carbon (8.3×10^{-4} mol L^{-1}) in the sample.

SWNTs, and this is apparent in much of the data in the tables and figures. Because this comparison of absorbances is taken at the peak of the SWNT interband transitions, it reflects the order of the SWNT diameters. Smaller diameter SWNTs absorb at higher energies and therefore sit higher on the sloping π-plasmon baseline. (The diameter of the SWNTs increases in the following order: HC < LO < EA.)

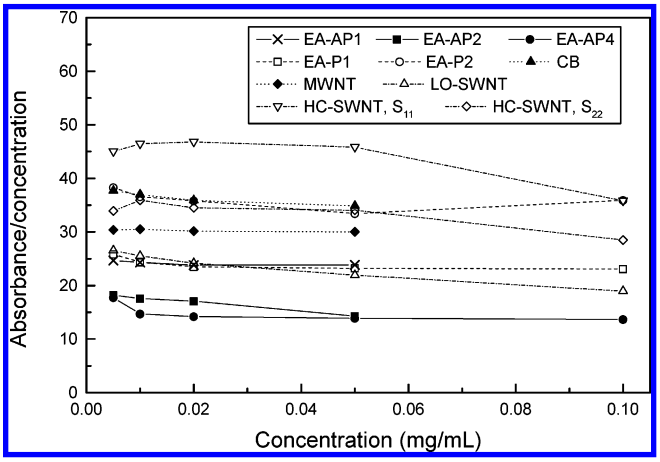

Figure 6. Plot of concentration versus absorbance (at 9850 cm^{-1}; 7560 cm^{-1} for HC-SWNT S_{11}, 13 450 cm^{-1} for HC-SWNT S_{22}, 10 450 cm^{-1} for LO-SWNT S_{22}) for the carbon materials.

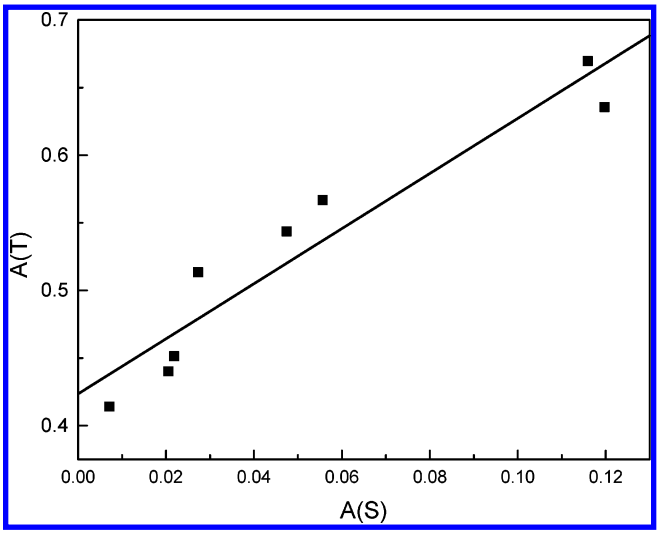

Figure 7. Plot of A(T, X) against A(S, X) for EA-AP samples and EA-P samples with a total carbon concentration of C(X) = 0.02 mg/mL (see eq 10); intercept = 0.423 ± 0.018, gradient = 2.0 ± 0.2, R^2 = 0.91, sd = 0.030.

Figures 7 and 8 show plots of A(T, X) against A(S, X) for six EA-AP(1−6) samples and the purified samples EA-P(2−3) with total carbon concentrations of C(X) = 0.02 and 0.01 mg/mL within the spectral cutoffs given in Table 1. The intercepts and gradients allow us to solve for the quantities in eq 10, and thus we obtain the absolute values of the molar extinction coefficients of the impurities present in EA-SWNTs: ϵ(I) =

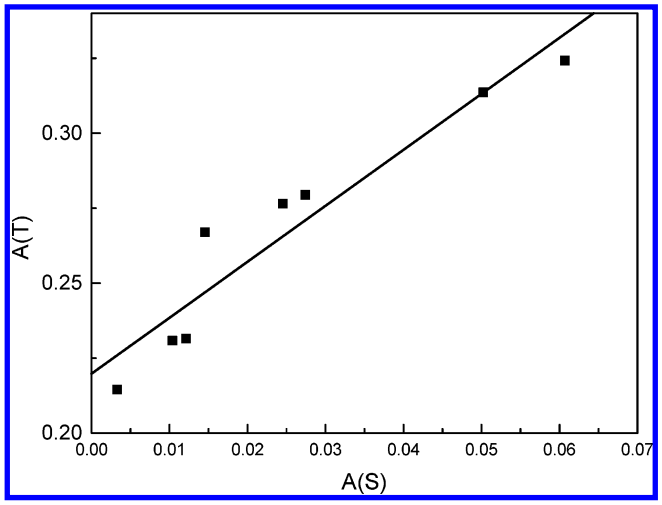

Figure 8. Plot of A(T, X) against A(S, X) for EA-AP samples and EA-P samples with a total carbon concentration of C(X) = 0.01 mg/mL (see eq 10); intercept = 0.220 ± 0.008, gradient = 1.9 ± 0.2, R^2 = 0.91, sd = 0.013.

254 ± 11 and 265 ± 10 L mol^{-1} cm^{-1}, respectively. The scatter in these graphs is due to a combination of experimental errors and variations in the composition of the impurities, and we take ϵ(I) = 260 ± 20 L mol^{-1} cm^{-1} at 9750 cm^{-1}. If we take the value of the gradient to be ~2 = {[ϵ(N) + ϵ(S) − ϵ(I)] × ϵ(S)$^{-1}$}, then ϵ(N) ≈ ϵ(S) + ϵ(I) = ϵ(S) + 260 L mol^{-1} cm^{-1} (all at 9750 cm^{-1}). Thus, the strength of the background π-plasmon absorption is somewhat greater in the SWNTs than in the impurities, presumably because of the disorder in the latter material.

The most important goal of our work is the development of an absolute scale of SWNT purity based on NIR spectroscopy, which requires the availability of an analytically pure SWNT sample. This in turn will allow the determination of the ratio of A(S,R)/A(T,R) for a pure SWNT sample (R) and thereby provide a reference against which an arbitrary sample may be measured.

Conclusions

We have demonstrated the applicability of Beer's law to the study of the solution-phase NIR spectroscopy of a variety of carbon materials at concentrations of 0.01 and 0.02 mg/mL in DMF. When the data were normalized for concentration, it was found that there is a correlation between the value of the absorbance and the purity of EA-SWNTs. An analysis of the data for a range of EA-SWNT samples of constant total concentration but varying purity allowed the following relationships to be derived: ϵ(I) = 260 ± 20 L mol^{-1} cm^{-1} and ϵ(N) ≈ ϵ(S) + ϵ(I) = ϵ(S) + 260 L mol^{-1} cm^{-1} (where ϵ(S) is the molar extinction coefficient due to the S_{22} interband transition of the EA-SWNTs, ϵ(N) is the molar extinction coefficient due to the π-plasmon transition of the SWNTs, and ϵ(I) is the molar extinction coefficient due to the π-plasmon transition of the impurities, all at 9750 cm^{-1}).

Acknowledgment. This work was supported by DOD/DARPA/DMEA under Award No. DMEA90-02-2-0216. Carbon Solutions, Inc. acknowledges NSF SBIR Phase I and II Awards No. DMI-0110221 from the Division for Design, Manufacture and Industrial Innovation and a DARPA Phase I SBIR administered by the U.S. Army Aviation and Missile Command (award no. W31P4Q-04-C-R171).

References and Notes

(1) Bandow, S.; Rao, A. M.; Williams, K. A.; Thess, A.; Smalley, R. E.; Eklund, P. C. *J. Phys. Chem. B* **1997**, *101*, 8839−8842.
(2) Rinzler, A. G.; Liu, J.; Dai, H.; Nilolaev, P.; Huffman, C. B.; Rodriguez-Macias, F. J.; Boul, P. J.; Lu, A. H.; Heymann, D.; Colbert, D. T.; Lee, R. S.; Fischer, J. E.; Rao, A. M.; Eklund, P. C.; Smalley, R. E. *Appl. Phys. A* **1998**, *67*, 29−37.
(3) Liu, J.; Rinzler, A. G.; Dai, H.; Hafner, J. H.; Bradley, R. K.; Boul, P. J.; Lu, A.; Iverson, T.; Shelimov, K.; Huffman, C. B.; Rodriguez-Macias, F.; Shon, Y.-S.; Lee, T. R.; Colbert, D. T.; Smalley, R. E. *Science* **1998**, *280*, 1253−1255.
(4) Chiang, I. W.; Brinson, B. E.; Smalley, R. E.; Margrave, J. L.; Hauge, R. H. *J. Phys. Chem. B* **2001**, *105*, 1157−1161.
(5) Jeong, T.; Kim, W.-Y.; Hahn, Y.-B. *Chem. Phys. Lett.* **2001**, *344*, 18−22.
(6) Moon, J. M.; An, K. H.; Lee, Y. H.; Park, Y. S.; Bae, D. J.; Park, G. S. *J. Phys. Chem. B* **2001**, *105*, 5677−5681.
(7) Vaccarini, L.; Goze, C.; Aznar, R.; Micholet, V.; Journet, C.; Bernier, P. *Synth. Met.* **1999**, *103*, 2492−2493.
(8) Dillon, A. C.; Gennett, T.; Jones, K. M.; Alleman, J. L.; Parilla, P. A.; Heben, M. J. *Adv. Mater.* **1999**, *11*, 1354−1358.
(9) Monthioux, M.; Smith, B. W.; Burteaux, B.; Claye, A.; Fischer, J. E.; Luzzi, D. E. *Carbon* **2001**, *39*, 1251−1272.
(10) Holzinger, M.; Hirsch, A.; Bernier, P.; Duesberg, G. S.; Burghard, M. *Appl. Phys. A* **2000**, *70*, 599−602.
(11) Gorelik, O. P.; Nikolaev, P.; Arepalli, S. *NASA CR-2000-208926* **2001**.
(12) Zhang, M.; Yudasaka, M.; Koshio, A.; Iijima, S. *Chem. Phys. Lett.* **2002**, *364*, 420−426.
(13) Hennrich, F.; Lebedkin, S.; Malik, S.; Tracy, J.; Barczewski, M.; Rosner, H.; Kappes, M. *Phys. Chem. Chem. Phys.* **2002**, *4*, 2273−2277.
(14) Itkis, M. E.; Perea, D.; Niyogi, S.; Rickard, S.; Hamon, M.; Hu, H.; Zhao, B.; Haddon, R. C. *Nano Lett.* **2003**, *3*, 309−314.
(15) Itkis, M. E.; Niyogi, S.; Meng, M.; Hamon, M.; Hu, H.; Haddon, R. C. *Nano Lett.* **2002**, *2*, 155−159.
(16) Liu, J.; Casavant, M. J.; Cox, M.; Walters, D. A.; Boul, P.; Lu, W.; Rimberg, A. J.; Smith, K. A.; Colbert, D. T.; Smalley, R. E. *Chem. Phys. Lett.* **1999**, *303*, 125−129.
(17) Niyogi, S.; Hamon, M. A.; Perea, D.; Kang, C. B.; Zhao, B.; Pal, S. K.; Wyant, A. E.; Itkis, M. E.; Haddon, R. C. *J. Phys. Chem. B* **2003**, *107*, 8799−8804.
(18) Zhou, B.; Lin, Y.; Li, H.; Huang, W.; Connell, J. W.; Allard, L. F.; Sun, Y. P. *J. Phys. Chem. B* **2003**, *107*, 13588−13592.
(19) Bahr, J. L.; Mickelson, E. T.; Bronikowski, M. J.; Smalley, R. E.; Tour, J. M. *Chem. Commun.* **2001**, 193−194.
(20) Hamon, M. A.; Hu, H.; Bhowmik, P.; Itkis, M. E.; Haddon, R. C. *Appl. Phys. A.* **2002**, *74*, 333−338.
(21) Clar, E. *Polycyclic Hydrocarbons*; Academic Press: London, 1964.